

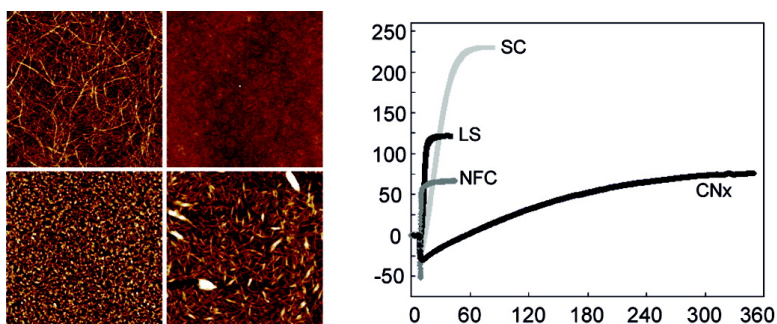
Article

Enzymatic Hydrolysis of Native Cellulose Nanofibrils and Other Cellulose Model Films: Effect of Surface Structure

S. Ahola, X. Turon, M. Osterberg, J. Laine, and O. J. Rojas

Langmuir, **2008**, 24 (20), 11592-11599 • DOI: 10.1021/la801550j • Publication Date (Web): 09 September 2008

Downloaded from <http://pubs.acs.org> on November 17, 2008



More About This Article

Additional resources and features associated with this article are available within the HTML version:

- Supporting Information
- Access to high resolution figures
- Links to articles and content related to this article
- Copyright permission to reproduce figures and/or text from this article

[View the Full Text HTML](#)



ACS Publications
High quality. High impact.

Langmuir is published by the American Chemical Society, 1155 Sixteenth Street N.W., Washington, DC 20036

Enzymatic Hydrolysis of Native Cellulose Nanofibrils and Other Cellulose Model Films: Effect of Surface Structure

S. Ahola,[†] X. Turon,^{*,‡,§} M. Österberg,[†] J. Laine,[†] and O. J. Rojas[‡]

Department of Forest Products Technology, Faculty of Chemistry and Materials Sciences, Helsinki University of Technology, P.O. Box 3320, FIN-02015 TKK, Espoo, Finland, and Forest Biomaterials Science and Engineering, College of Natural Resources, North Carolina State University, Campus Box 8005, Raleigh, North Carolina 27695-8005

Received May 20, 2008. Revised Manuscript Received July 2, 2008

Model films of native cellulose nanofibrils, which contain both crystalline cellulose I and amorphous domains, were used to investigate the dynamics and activities of cellulase enzymes. The enzyme binding and degradation of nanofibril films were compared with those for other films of cellulose, namely, Langmuir–Schaefer and spin-coated regenerated cellulose, as well as cellulose nanocrystal cast films. Quartz crystal microbalance with dissipation (QCM-D) was used to monitor the changes in frequency and energy dissipation during incubation at varying enzyme concentrations and experimental temperatures. Structural and morphological changes of the cellulose films upon incubation with enzymes were evaluated by using atomic force microscopy. The QCM-D results revealed that the rate of enzymatic degradation of the nanofibril films was much faster compared to the other types of cellulosic films. Higher enzyme loads did not dramatically increase the already fast degradation rate. Real-time measurements of the coupled contributions of enzyme binding and hydrolytic reactions were fitted to an empirical model that closely described the cellulase activities. The hydrolytic potential of the cellulase mixture was found to be considerably affected by the nature of the substrates, especially their crystallinity and morphology. The implications of these observations are discussed in this report.

Introduction

The reduced availability of nonrenewable resources has triggered interest to produce materials and energy from cellulose, the most abundant and sustainable polymer in the biosphere. In order to supply biofuels as an alternative source of energy, enzymatic hydrolysis can be utilized to produce the required fermentable sugars from cellulose. However, the conversion of lignocellulosics to monomeric sugars is a complex process. The substrate's chemistry, heterogeneity, crystallinity, and surface area strongly affect the kinetics of the enzymatic conversion. Fundamental studies on the enzyme–substrate interactions are contributing to develop more effective enzyme mixtures. Cellulases are enzymes that are used in many industrial applications (including food processing, textiles, pulp and paper, etc.) by taking advantage of their ability to hydrolyze β -(1–4)-bonds in cellulose. A complete enzymatic hydrolysis of cellulose chains to glucose is accomplished with the complementary activity of different cellulases. Cellulases are divided into three different categories:¹ endo-1,4- β -glucanases (EGs) that target cellulose chains in random locations away from the chain ends; exoglucanases or exocellobiohydrolases (CBHs) that degrade cellulose by splitting off molecules from both ends of the chain producing cellobiose dimers; and β -glucosidases (BGLs) that hydrolyze the cellobiose units (produced during EG and CBH attack) to glucose. While each component in cellulase systems play individual roles, it is important to recognize that the overall effect observed in cellulose degradation is a combined, synergistic interaction between the various enzyme components.

A cost-effective conversion of cellulose via enzymatic fermentation requires detailed knowledge of the surface chemistry of the available forms of cellulose and the specific interactions between the enzymes and these substrates. To this end, mechanistic aspects such as cellulase binding and substrate degradation have recently been studied using model films of regenerated cellulose in combination with electromechanical and optical sensing techniques.^{2–5} In a recent paper, Josefsson et al.⁴ studied the effect of different cellulases on cellulose II model films. Their results indicated that EGs produce swelling and the development of new end groups in the cellulose substrate. On the other hand, CBHs degraded the cellulose films rather fast. However, it is widely known that multicomponent cellulases can produce cellulose degradation at significantly higher rates due to the synergistic effects of the different constituents. It has become apparent that the mechanism of enzymatic cellulose degradation is extremely complex. Besides molecular factors and physical-chemical conditions, the enzyme activity depends on the properties of the cellulose substrate, including its morphology, composition, degree of polymerization, crystallinity (recalcitrance), and accessible surface area.^{4,6–10} It is widely accepted that the

* Corresponding author. Telephone: 9195137884. Fax: 9195156302. E-mail: xtcasipr@ncsu.edu.

[†] Helsinki University of Technology.

[‡] North Carolina State University.

[§] Current address: Bioengineering Department, Institut Químic de Sarrià, Universitat Ramon Llull, 08017 Barcelona. E-mail: xavier.turon@iqs.edu. Phone: 932672000; Fax: 932056266.

(1) Rabinovich, M. L.; Melnick, M. S.; Bolobova, A. V. *Biochemistry (Moscow)* **2002**, *67*, 850–871.

(2) Turon, X.; Rojas, O. J.; Deinhammer, R. S. *Langmuir* **2008**, *24*(8), 3880–3887.

(3) Rojas, O. J.; Jeong, C.; Turon, X.; Argyropoulos, D. S. In *Measurement of Cellulase Activity with Piezoelectric Resonators: Materials, Chemicals and Energy from Forest Biomass*; ACS Series 954; Oxford University Press: Washington, DC, 2007; pp 478–494.

(4) Josefsson, P.; Henriksson, G.; Wågberg, L. *Biomacromolecules* **2008**, *9*, 249–254.

(5) Eriksson, J.; Malmsten, M.; Tibergh, F.; Callisen, T. H.; Damhus, T.; Johansen, K. S. *J. Colloid Interface Sci.* **2005**, *284*, 99–106.

(6) Jeoh, T.; Wilson, D. B.; Walker, L. P. *Biotechnology Progress* **2006**, *22*, 270–277.

(7) Himmel, M.; Ding, S.; Johnson, D.; Adney, W.; Nimlos, M.; Brady, J.; Foust, T. *Science* **2007**, *315*, 804–807.

(8) Fierobe, H.; Bayer, E.; Tardif, C.; Czjzek, M.; Mechaly, A.; Belaich, A.; Lamed, R.; Shoham, Y.; Belaich, J. *J. Biol. Chem.* **2002**, *277*, 49621–49630.

(9) Woodward, J.; Affholter, K. A.; Noles, K. K.; Troy, N. T.; Gaslightwala, S. F. *Enzyme Microb. Technol.* **1992**, *14*(8), 625–630.

(10) Béguin, P.; Aubert, J. *FEMS Microbiol. Rev.* **1994**, *13*(1), 25–58.

crystalline regions are more difficult to degrade by the enzymes than the amorphous ones.^{7,11} However, this aspect has not been taken into account in previous model film studies on enzymatic degradation. Thin films of cellulose used in related studies have been produced from cellulose suspensions that led to (regenerated) amorphous cellulose. Solubilization of cellulose I in a solvent, such as *N*-methylmorpholine-*N*-oxide (NMMO), followed by reprecipitation results in antiparallel cellulose II structure.¹² In contrast, native cellulose consists of crystalline cellulose I interposed in amorphous structures of the cell wall. Since the cellulose suprastructure strongly affects the functions of the cellulase enzymes it would be essential to study ensuing interactions using a more representative substrate for native cellulose, i.e., one containing both crystalline cellulose I and amorphous regions.

In this contribution we propose the use of native cellulose nanofibrils for elucidation of enzyme activities at the nanoscale by using quartz crystal microbalance with dissipation (QCM-D) and atomic force microscopy (AFM). Cellulose microfibrils are substructural elements of cellulosic fibers that can be mechanically disintegrated from the cell wall matrix.^{13,14} Novel enzymatic¹⁵ or chemical,^{16–18} pretreatments combined with mechanical disintegration of the fibers produce robust, homogeneous, nanoscale fibril materials, which are promising for many nanotechnology applications.^{15,19,20} Noteworthy, the size and nature of these native cellulose nanofibrils make these structures amenable to the manufacture of robust thin films for further investigation. In a recent paper by Ahola et al.,²⁰ native cellulose model films containing both crystalline cellulose I and amorphous regions, and some residual hemicelluloses, were prepared by spin-coating aqueous cellulose nanofibril suspensions onto silica substrates. It was found that these films were smooth and stable in aqueous solutions and they were used successfully to study swelling and surface interactions by QCM-D and AFM, respectively.

Modeling the kinetics of enzyme–substrate interactions is crucial to allow a good comparison of results using various substrates, enzymes, or experimental conditions. Various kinetic models have been developed to describe the hydrolysis rate by cellulases. Most models, based on reactor dynamics, involve the quantification of the hydrolysis rate from the (known) concentrations of available cellulose substrate and enzyme in solution. Typical models include the Michaelis–Menten equation.^{21,22} Studies performed using the QCM-D allows real-time monitoring of the interactions between the enzymes and the substrate; however, in contrast to the case of substrates in the dispersed (or colloidal) state, QCM-D is typically limited to flat, homogeneous

films that are fixed onto the respective resonator. In this case, the “concentration” of the substrate is not a relevant parameter in any kinetic model to be applied. From these considerations, classical, deterministic kinetic models could not be applied and other quantification approaches are required, such as that presented in an earlier report by the authors.²

In summary, in this study we used native cellulose nanofibril films as those reported by Ahola et al.²⁰ to unveil details of their enzymatic hydrolysis upon incubation in cellulase enzyme mixtures. The effect of the substrate structure was studied in terms of its susceptibility to cellulolytic hydrolysis. For this purpose we employed a commercial cellulase mixture since it is the combined effect of different cellulases that is responsible for maximum conversion rates in actual applications. Our results on enzyme binding and substrate degradation were compared with three other types of models for cellulose, namely, Langmuir–Schaefer (LS) and spin-coated regenerated cellulose (SC), as well as cellulose nanocrystal cast (NC) film. Finally, an empirical model based on QCM-D data² was used to quantify and compare the enzyme binding and hydrolysis rates for all the model films investigated.

Experimental Section

Preparation of Cellulose Nanofibril Model Films. Cellulose nanofibrils were disintegrated from delignified sulfite pulp by using a high-pressure fluidizer (Microfluidizer M-110EH, Microfluidics Corp., Newton, U.S.) at STFI-Packforsk, Stockholm, Sweden.¹⁵ The 2% nanofibril gel was diluted with water from Milli-Q Gradient system (resistivity > 18 M Ω) to 1.67 g/L and centrifuged for 45 min at 10400 rpm (10 000 G) to remove remaining fibril aggregates using an Optima L-90K ultracentrifuge from Beckman Coulter, U.S.A. The clear supernatant was used for spin-coating. The concentration of nanofibrils in the supernatant was 0.4 g/L. Substrates used for model surface preparation were silica QCM-D crystals (Q-sense AB, Västra Frölunda, Sweden). Silica substrates were washed by immersing the crystals in 10% NaOH solution, after which the crystals were rinsed with Milli-Q water, dried with nitrogen gas, and placed in a UV/ozone oven for 15 min. 3-Aminopropyltrimethoxysilane (APTS) was adsorbed onto the silica substrates in order to improve the coverage of the nanofibrils. Washed silica substrates were immersed into 1% v/v APTS/toluene solution for 40 min, rinsed with toluene and dried in an oven at 60 °C for 30 min. The model films were prepared by spin-coating the nanofibril dispersion onto the substrates at 3000 rpm for 45 s. The spin-coated surfaces were rinsed with water, dried gently with nitrogen gas and heat-treated in an oven at 80 °C for 10 min. The preparation of the nanofibril films is presented in more detail elsewhere.²⁰

Preparation of LS Cellulose Films. Substrates used for LS-film preparation were QCM-D crystals, which were spin-coated with polystyrene by the supplier (Q-sense AB, Gothenburg, Sweden). Trimethylsilyl cellulose (TMSC) was deposited on the polystyrene-coated crystals using the horizontal LS deposition technique. The preparation of films is presented in a previous work.²³ Prior to use in QCM-D, TMSC deposited on the polystyrene crystal was converted to cellulose by desilylation using hydrochloric acid vapor.²⁴

Cellulose NC Films. Cellulose nanocrystals were obtained by HCl acid hydrolysis of Whatman cellulose filter paper.²⁵ A 700 mL portion of 1.5 M HCl was added to 20 g of filter paper, and the cellulose was hydrolyzed at 100 °C for ca. 4 h after being ground by a 10-Speed Osterizer Blender (Oster, U.S.A.). After the hydrolysis, the cellulose solution was diluted with deionized water and

(11) Teeri, T. T. *Trends Biotechnol.* **1997**, *15*, 160–167.

(12) O'Sullivan, A. *Cellulose* **1997**, *4*, 173–207.

(13) Turbak, A. F.; Snyder, F. W.; Sandberg, K. R. *J. Appl. Polym. Sci.: Appl. Polym. Symp.* **1983**, *37*, 815–827.

(14) Herrick, F. W.; Casebier, R. L.; Hamilton, J. K.; Sandberg, K. R. *J. Appl. Polym. Sci.: Appl. Polym. Symp.* **1983**, *37*, 797–813.

(15) Pääkko, M.; Ankerfors, M.; Kosonen, H.; Nykänen, A.; Ahola, S.; Österberg, M.; Ruokolainen, J.; Laine, J.; Larsson, P. T.; Ikkala, O.; Lindström, T. *Biomacromolecules* **2007**, *8*, 1934–1941.

(16) Saito, T.; Nishiyama, Y.; Putaux, J.; Vignon, M.; Isogai, A. *Biomacromolecules* **2006**, *7*, 1687–1691.

(17) Abe, K.; Iwamoto, S.; Yano, H. *Biomacromolecules* **2007**, *8*, 3276–3278.

(18) Wågberg, L.; Decher, G.; Norgren, M.; Lindström, T.; Ankerfors, M.; Axnäs, K. *Langmuir* **2008**, *24*, 784–795.

(19) Berglund, L. In *Natural Fibers, Biopolymers, and Biocomposites*; Mohanty, A., Misra, M., Drzal, L., Eds.; CRC Press: Boca Raton, FL, 2005; pp 807–832.

(20) Ahola, S.; Salmi, J.; Johansson, L. S.; Laine, J.; Österberg, M. *Biomacromolecules* **2008**, *9*, 1273–1282.

(21) Rosenau, T.; Potthast, A.; Sixta, H.; Kosma, P. *Prog. Polym. Sci.* **2001**, *26*(11), 1763–1837.

(22) Ramos, L. P.; Breuil, C.; Saddler, J. N. *Enzyme Microb. Technol.* **1993**, *15*, 19–25.

(23) Tammelin, T.; Saarinen, T.; Österberg, M.; Laine, J. *Cellulose* **2006**, *13*, 519–535.

(24) Schaub, M.; Wenz, G.; Wegner, G.; Stein, A.; Klemm, D. *Adv. Mater.* **1993**, *5*, 919–922.

(25) Kim, J.; Montero, G. A.; Wang, X.; Argyropoulos, D. S.; Genzer, J.; Hinestroza, J. P.; Rojas, O. J. High-Performance Nanofibers and Nanostructures for New Generation Multifunctional Materials. Presented at the 2006 AIChE Annual Meeting, San Francisco, CA, 2006.

centrifuged at 2800 rpm, whereupon the clear upper phase of acid was removed. After rinsing four to five times with water, the cellulose nanocrystals were dispersed in water. The collected turbid solution was further centrifuged at 8000 rpm for 30 min and then at 14 000 rpm for the following 30 min. Very fine particles in the upper phase were removed, and the deposits after the high speed centrifugation were freeze-dried using a Labconco system (Kansas City, MO).

Silica QCM-D sensors were cleaned (UV-ozone plus alkali treatment), immersed in poly(vinylamine) (PVAm) solution for more than 30 min and then rinsed with Milli-Q water. A drop of cellulose nanocrystal aqueous dispersion was deposited on the PVAm-coated surface. Then the surface was rinsed with Milli-Q water and dried in an oven at 80 °C for 1 h.

SC Films. Microcrystalline cellulose (Avicel) was dissolved in 50% NMMO at 115 °C. Dimethyl sulfoxide (DMSO) was added to adjust the concentration of the polymer (0.05%) and viscosity of the mixture. Cleaned gold QCM-D sensors were immersed in PVAm solution for more than 10 min and then rinsed with Milli-Q water and dried. A drop of the cellulose solution was deposited on the surface to create a uniform thin film via the spin coating technique. The substrate was dried in an oven at 80 °C for two hours and then washed thoroughly with Milli-Q water.²⁶

Enzyme Solution. The enzyme used in this work was a commercial cellulase mixture, NS50013 cellulase complex from Novozymes (Celluclast™), which is available as an aqueous solution (≥ 700 U/g and an activity of 68 FPU/g). This commercial enzyme mixture obtained from *Trichoderma reesei* fungus contains EGs, CBHs, and BGLs. This mixture is formulated for the efficient saccharification of lignocellulosic materials, and its use is widely reported.^{22,27–29} The enzyme mixture has a maximum activity in mild acidic conditions (pH of ca.5), and temperatures between 50–60 °C. Sodium acetate, sodium hydroxide, sodium chloride, and acetic acid (all from Fisher Scientific) were used in the preparation of pH 5 buffer solutions. The ionic strength used in all experiments was kept at 0.1 M, and all solutions were prepared with Milli-Q water.

AFM Imaging. AFM imaging was used to characterize the changes in the structure and morphology of the cellulose model films, before and after enzymatic hydrolysis, using a Nanoscope IIIa Multimode scanning probe microscope from Digital Instruments Inc. (Santa Barbara, CA). The reference samples of the cellulose model films were immersed in buffer solution for at least 2 h, rinsed with Millipore water, dried with nitrogen gas and placed into a desiccator overnight before imaging. The enzymatically hydrolyzed samples were taken out of the QCM-D chambers (see below), rinsed, dried, and placed into a desiccator overnight. The images were acquired using tapping mode in air with silicon cantilevers (NSC15/AIBS) delivered by MicroMasch, Tallinn, Estonia. The drive frequency of the cantilever was 310–345 kHz. Scanning sizes of $1 \times 1 \mu\text{m}$ or $5 \times 5 \mu\text{m}$ were conducted on at least three different areas of each sample. No image processing except flattening was made. The root-mean-square (rms) roughness was determined over a $25 \mu\text{m}^2$ area using the Nanoscope software.

Enzyme–Cellulose Surface Interactions Studied by QCM-D. A QCM-D (Q-sense AB model E-4, Västra Frölunda, Sweden) was used to study enzyme binding and activity on the cellulose thin films deposited on the sensors. The temperature in our experiments was varied between 20 and 40 (± 0.02) °C using a Peltier element built in the QCM apparatus. In a typical experiment, buffer solution was injected into the QCM flow module where the cellulose-coated QCM resonator was mounted. The coated sensor remained in contact with the background electrolyte solution to allow the cellulose film to fully swell and reach equilibrium with the medium (as confirmed with a constant QCM frequency signal or baseline). Afterwards, enzyme solution was continuously introduced into the QCM cell

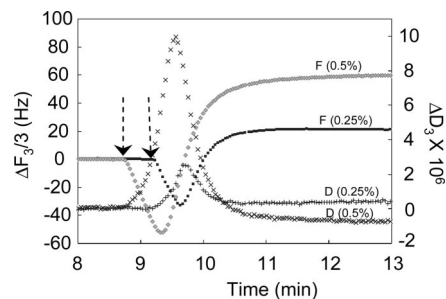


Figure 1. Change in frequency (Δf) for cellulose nanofibril surface treated with 0.5% cellulase mixture (gray diamonds) and 0.25% cellulase mixture (dark squares); and respective change in dissipation (ΔD) (in x's and crosses for 0.5% and 0.25% cellulase mixture, respectively). The frequency and dissipation profiles are the normalized third overtones for a driving frequency of 15 MHz (40 °C and pH 5). Frequency decreases as enzymes bind to the nanofibril surface and increases when hydrolysis is dominating. A maximum in the ΔD curves is detected during the hydrolysis phase. The time at which the surfaces were exposed to enzymes is indicated by the arrows.

with a peristaltic pump at a flow rate of 0.2 mL/min. The experiments reported here were conducted in *batch* conditions. In this mode of operation, the enzyme solution was introduced in the cell while ensuring that the buffer solution present initially was fully replaced (a minimum exchange of six cell volume-equivalents were carried out in each run). In each experiment, enzyme solution was injected only after ensuring that the drift of the third overtone frequency (Δf_3) for the cellulose-coated sensor in background electrolyte solution was lower than 2 Hz per hour. This was taken as an indication of a full stabilization of the film in the buffer solution (fully swelled film and stress-free system). Enzyme incubation was terminated when no appreciable changes in frequency were observed.

Binding and Hydrolysis Dynamics. In order to fit key kinetic parameters to the experimental results, eqs 1 and 2 were used to model binding and hydrolytic activity, respectively. These equations and the significance of the respective fitting parameters are explained in more detail elsewhere.²

$$\Delta f = M_{\text{MAX}} \left(1 - e^{-\frac{t}{\tau}} \right) \quad (1)$$

$$\Delta f = A + \frac{B - A}{\left(1 + e^{\frac{V_{50} - t}{C}} \right)} \quad (2)$$

Δf and t in eqs 1 and 2 are the frequency variation (Hz) and experimental time (min), respectively. The binding parameters shown in eq 1 include M_{MAX} , the maximum binding value in Hz (corresponding to the minimum frequency measured, or plateau value) and τ , the relaxation time or the reciprocal of the enzyme adsorption rate, expressed in min^{-1} .

The parameters that describe the hydrolytic activity in eq 2 include B , the maximum frequency change (Hz), which corresponds to the plateau in the QCM signal once degradation is completed (see, for example, Figure 1). It also includes V_{50} , the time (min) at which the inflection in frequency profile occurs; C , the reciprocal of the hydrolysis rate (min^{-1}) and parameter A that corresponds to the minimum frequency (Hz) in the respective profile (not relevant to the kinetic analysis).

Results and Discussion

Enzymatic Hydrolysis of Cellulose Nanofibril Films. The adsorption of the cellulase mixture on cellulose nanofibril model surfaces, the kinetics of enzyme binding, and substrate degradation were studied using QCM-D. The effect of temperature on the enzymatic degradation was studied by running the experiments in the 20–40 °C range. In addition, the effect of enzyme concentration was studied by varying the cellulase load between 0.01% and 0.5% (v/v).

(26) Fält, S.; Wägberg, L.; Vesterlind, E. L.; Larsson, P. T. *Cellulose* **2004**, *11*, 151–162.

(27) Bezerra, R. M. F.; Dias, A. A. *Appl. Biochem. Biotechnol.* **2005**, *126*, 49–60.

(28) Breuil, C.; Chan, M.; Gilbert, M.; Saddler, J. N. *Bioresour. Technol.* **1992**, *39*, 139–142.

(29) Yang, B.; Wyman, C. E. *Biotechnol. Bioeng.* **2006**, *94*, 611–617.

The enzymatic degradation of the nanofibril films was found to be an extremely fast process for all incubation temperatures used, including the 20 °C case. We note that faster rates of hydrolysis were observed at higher temperatures, as expected. Compared to the effect of enzyme load (to be presented in a later section), the incubation temperature was found to be less important (in the temperature range investigated) as far as the total hydrolysis rate is concerned. Hence, we gave emphasis to the effect of enzyme concentration in further degradation studies with nanofibril films. The effect of enzyme load on the extension and rate of protein binding was studied thereafter at a constant temperature (40 °C).

Experiments were conducted using different cellulase concentrations between 0.01% and 0.5% (v/v) in acetate buffer solution at pH 5.0, which is the optimum pH for the enzyme mixture employed. On the basis of the available cellulose surface area, all the concentrations used were well in excess of the required dose for full enzyme coverage. Fast enzyme binding to the surface is detected soon after introducing the cellulase solution in the QCM cell, see Figure 1. An increased concentration of cellulase leads to a larger reduction in resonator frequency, which is an indication of a larger enzyme adsorption. At a certain time after injection, which was usually less than one minute, the trend in frequency is reversed and it starts to increase. At this point the hydrolysis of the substrate dominates over binding as cellulase enzymes start to degrade the available cellulose.² It is worth noting that the total mass and thickness of the cellulose films used to measure the changes in frequency and dissipation presented in Figure 1 were different (slightly different amounts of fibrils were deposited on the sensors), and therefore the total released mass (and the limiting Δf at 13 min time) was also different. The observed changes in energy dissipation confirm the events described earlier: Initially a sharp increase in dissipation is detected, which is explained by enzyme binding and the onset of their activity. Soon thereafter, a maximum in energy dissipation is reached. This maximum dissipation occurs around the time when the hydrolysis rate starts to slow down (see Figure 1).

A distinctive characteristic of the native cellulose nanofibril films is the extremely high rate of hydrolysis, as judged by the frequency profiles shown in Figure 1. The time required for complete substrate degradation after enzyme injection was typically less than five minutes. This is very fast when compared to results reported for other substrates² or when compared with experiments with films of regenerated and nanocrystalline cellulose, as will be discussed later.

The nanofibrils have both crystalline and amorphous regions. The degree of crystallinity for nanofibrils is believed to be rather low.¹⁵ These facts favor a faster enzymatic degradation, yet they may not be enough to explain the comparatively faster dynamics observed for films of nanofibrillar cellulose. Two possible causes for the observed rapid hydrolysis are proposed: First, the nanofibrillar films have a distinctive high surface area available for enzyme binding and subsequent hydrolysis, and, second, EGs are expected to attack sections of the nanofibrils (preferably amorphous ones), close to the anchoring substrate, promoting whole sections of the fibrils to be cleaved. As a result, a fast release from the surface (and ensuing large increase in QCM frequency) is observed. Hence, the mass released, as detected by QCM's Δf may not be due to complete degradation of the cellulose film (e.g., to oligomers, cellobiose, or sugars). It is important to note that there was no indication of the release of the film because of a weak binding with the resonator surface (which would arguably be an alternate explanation for the fast dynamics observed). On the contrary, evidence shows that the films were

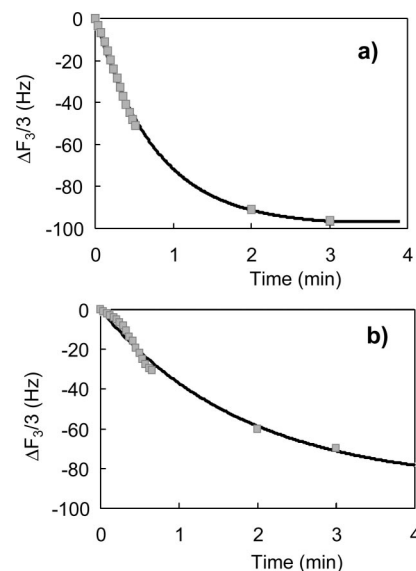


Figure 2. Fitted frequency (solid line) according to experimental data (square symbols) after enzyme binds to the nanofibril film at 40 °C with an enzyme load of 0.5% v/v (a) and 0.25% v/v (b). Note the short time span in these plot (up to 4 min after enzyme injection at 0 min time).

very robust and a strong binding existed between the films and the sensor surface. Furthermore, all the profiles in QCM frequency and dissipation that were acquired rule out such alternative. In sum, the degradation mechanism involved in the case of nanofibrillar films indicates the release of accessible fractions of cellulose chains (an event that is likely to occur in the case of whole lignocellulosic substrates).

Binding and Hydrolysis Dynamics Analysis for the Cellulose Nanofibril Films. Detection of enzyme binding on cellulose by using QCM-D is challenging due to the superimposed effect of substrate hydrolysis. In this section, the correlation between mass transfer and hydrolysis' dynamics will be highlighted. While the effect of enzyme concentration could be clearly elucidated from the experimental results, modeling helps us to quantify and compare the kinetic parameters for the different substrates (or for different experimental conditions). However, our aim in applying the respective kinetic models is not to describe the detailed molecular mechanisms occurring at the surface. Concurrent and complex phenomena and mechanisms occur during binding and hydrolysis, and therefore our model is simply used to describe the overall event, which allows us to quantify and to draw meaningful comparisons of enzymatic activities on the different substrates. It is also noteworthy that the experiments performed with QCM-D using enzymes reflect a dynamic equilibrium between enzyme adsorption and desorption between surface and the bulk phase. This also includes the fact that enzymes present in the bulk fluid can bind on partially degraded cellulose film for further degradation. It is therefore expected, as pointed out in earlier discussions² that binding, swelling, and hydrolysis phases are somewhat superimposed.

Equation 1 was used to fit the experimental data in the initial stage upon enzyme injection, as presented in Figure 2. A fast enzyme binding to the nanofibril surface was detected when injecting the solution containing cellulases. Increased concentration of cellulase led to a larger decrease in frequency. At a certain time (typically less than 1 min) the frequency trend was reversed, i.e., the frequency increased.

The experimental results for the hydrolytic phase for the nanofibril films were modeled using eq 2. Figure 3 presents the

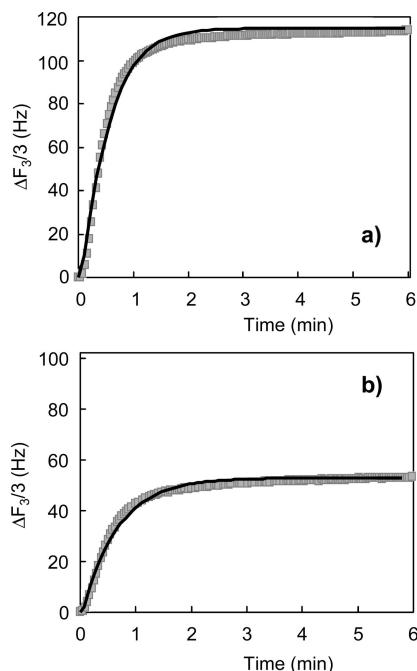


Figure 3. Experimental values (filled squares) and best fit using eq 2 for hydrolytic activity fitted (solid line) for frequency after enzymes bind to the nanofibril film at 40 °C with an enzyme load of (a) 0.5% v/v and (b) 0.25% v/v.

Table 1. Average Binding and Hydrolysis Parameters from Frequency Data for Cellulose Nanofibril Films after Treatment with Cellulases at Different Concentrations from 0.5 to 0.01% v/v and 40 °C

conc. (%)	0.50%	0.25%	0.05%	0.01%
M_{MAX} (Hz)	−95	−70	−34	−28
τ (min ^{−1})	0.7	1.3	1.7	1.0
B (Hz)	115	59.8	55.3	56.3
C (min ^{−1})	0.45	0.62	1.75	2.63
$1/C$ (min)	2.22	1.61	0.57	0.38

dynamics of hydrolysis brought about by the cellulase action, both experimental data and the best fit. The rate of hydrolysis of cellulose nanofibrils was found to be surprisingly fast if compared with other films of cellulose with similar thicknesses.²

Table 1 summarizes the average values for binding parameters (M_{MAX} and relaxation time τ) and the average values for hydrolysis parameters (B and C) for the set of enzyme concentrations tested. The M_{MAX} is related to the maximum amount of protein adsorbed, while the relaxation time quantifies (the inverse of) the rate of binding. The parameter B is a measure for the maximum extent of hydrolysis, or the total amount of enzymatically hydrolyzable cellulose. This parameter is proportional to the total mass of the film and is also influenced by the enzyme load when low amounts of enzyme are not able to totally degrade the film. The C value, the inverse of the hydrolysis rate, allows quantification and comparison of kinetic parameters from different experiments.

The highest concentration of cellulases (0.5% v/v) showed a markedly higher binding (larger M_{MAX}) (see Figure 2 and Table 1). Also, it is possible to confirm that, at higher enzyme loads, adsorption occurs faster (smaller τ). M_{MAX} values show an exponential relationship with enzyme concentration. At the highest enzyme concentration, the binding degree seems to reach a limiting value, which is expected because of the available surface area and its saturation with bound protein. With the exception of the data at the lowest enzyme load, the general trend for the binding rate, as quantified by the inverse of τ , is

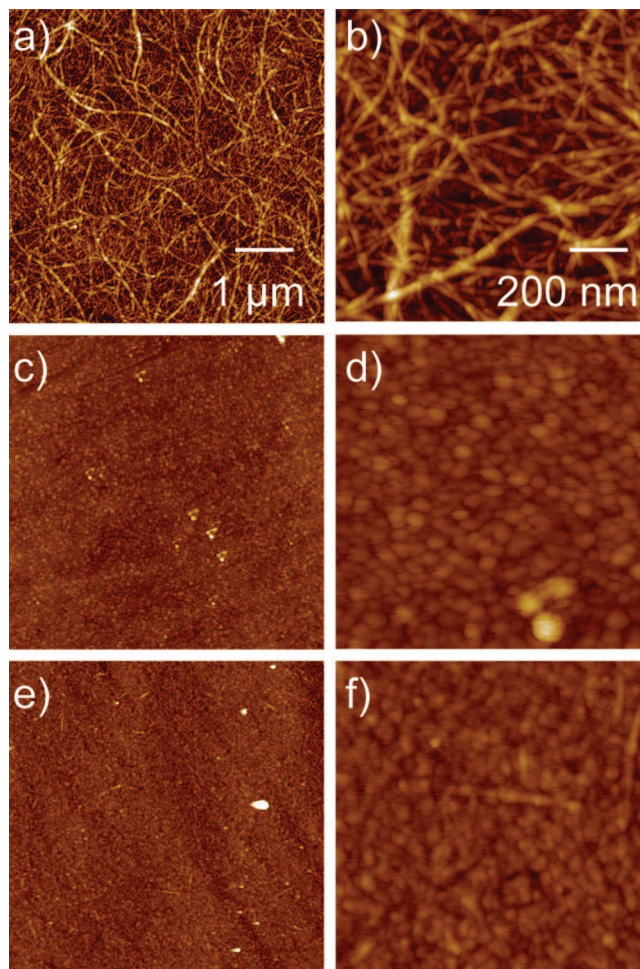


Figure 4. AFM height images of nanofibril model surfaces before (a,b) and after (c–f) enzymatic hydrolysis. The concentration of the enzyme in the hydrolysis was 0.5% (c,d) and 0.01% (e,f). The image size is 5 × 5 μm (a,c,e) and 1 × 1 μm (b,d,f). Z-range is 30 nm. The incubation time was <10 min (see Figure 1).

a linear increase with the enzyme concentration in this range of concentrations.

The hydrolysis rate ($1/C$) (see eq 2) is proportional to enzyme load, as shown in Table 1. The $1/C$ value for 0.5% mixture (compared to 0.25%) reveals that halving the concentration causes a 38% decrease in the hydrolysis rate. When diluted 10 times, the hydrolysis rate falls almost 4-fold. Finally, the enzyme dilution of 1:50 causes a 6-fold reduction of the hydrolysis rate. As mentioned before, the enzyme load affects drastically the dynamics of hydrolysis.

Changes in the Structure of Nanofibril Film after Enzymatic Hydrolysis. The structural and morphological changes suffered by the nanofibril films upon enzymatic treatment were followed with AFM imaging. Figure 4 shows reference height images (Figure 4 a,b) of nanofibrils covering the silica substrate. The topographic image of the nanofibril film (Figure 4a,b) shows an apparent high surface area, which is readily accessible to the enzymes. This is in contrast to the flat films of cellulose produced by spin coating or LS deposition. After enzymatic hydrolysis (40 °C, pH 5, cellulase concentration 0.01% and 0.5%), the nanofibril film is removed, and the typical structure of the substrate is revealed (Figure 4c–f). In the case of the lowest enzyme concentration (0.01%), some remaining rod-like fibrils can be seen on the surface (Figure 4e, f). These structures may be highly crystalline cellulose nanofibrils, which are difficult to degrade.

Table 2. Thickness and rms Roughness Values for NFC, LS, SC, and NC Cellulose Model Films

surface	thickness, nm	roughness (rms), nm
NFC film	10	3.3
LS film	10–15	0.9
SC film	30–35	5.1
NC film	20–30	10.2

As was pointed out in previous sections, the QCM-D results showed that the degradation of the nanofibril films was very fast. AFM images also suggest that despite the short time it takes for the degradation to occur, the nanofibril film is indeed completely removed.

Enzymatic Hydrolysis of Different Cellulose Model Films: A Comparison. In order to investigate the effect of the chemistry and structure of different cellulose model films on enzymatic hydrolysis, three additional types of cellulose films were used: LS regenerated cellulose, SC regenerated cellulose, and cast cellulose NC films. The extent of enzyme adsorption and dynamics of binding and substrate degradation was compared for all the films by using QCM-D. The main difference between these films was the degree of crystallinity and the crystalline form of cellulose. As already mentioned, cellulose nanofibril films contain both crystalline cellulose I and amorphous regions. LS and SC regenerated cellulose films are mainly amorphous, but may also contain crystalline cellulose II regions, as recently found in an ongoing X-ray diffraction study performed by the authors from TKK and their collaborators. Furthermore, LS films have a self-assembled-layer structure while the SC films are organized randomly. NC films entail a fully crystalline cellulose I structure. It is also noteworthy that the degradable mass is different for the four samples because of the differences in the film preparation procedures, and varying particle size of the cellulose materials. Table 2 lists thickness and roughness values for all the cellulose films studied. The thickness values for nanofibril, LS, and SC films were taken from refs 20, 23, and 26, respectively. The thickness of the NC film was determined using AFM imaging. All the rms roughness values were determined by AFM image analysis. The thicknesses of the nanofibril and LS films are similar, but the nanofibril film has higher rms roughness. SC and NC surfaces are thicker. However, the NC surface is distinctively rough. The average height of the nanocrystals was determined to be 20–30 nm using AFM image analysis, but the largest aggregates were up to 50 nm high, when two nanocrystals aggregated vertically.

As hydrolysis rates for LS, SC, and NC cellulose films were found to be much slower compared to nanofibril films, the 0.5% enzyme load was selected as the reference concentration to minimize the experimental time. Figure 5 shows the change in resonance frequency and energy dissipation for (a) NFC, (b) LS, (c) SC, and (d) NC cellulose films after incubation with 0.5% cellulase concentration at 40 °C. As cellulases are incubated, a typical fast decrease of frequency is detected. Such frequency decrease is related to the increase in mass as cellulases are rapidly bound to the surface. After incubation, the frequency increases, indicating mass release from the surface when cellulose hydrolysis becomes the dominant effect. These phases can be detected for all the model films studied, but the respective kinetics differs significantly.

The degradation time, i.e., the time between the point where frequency reaches the minimum value and the point where frequency reaches the plateau, varies greatly between the four films studied. When compared to nanofibril film (Figure 5a), it is evident that the degradation of the LS film (Figure 5b) is slower. The time required for film exhaustion or depletion in the

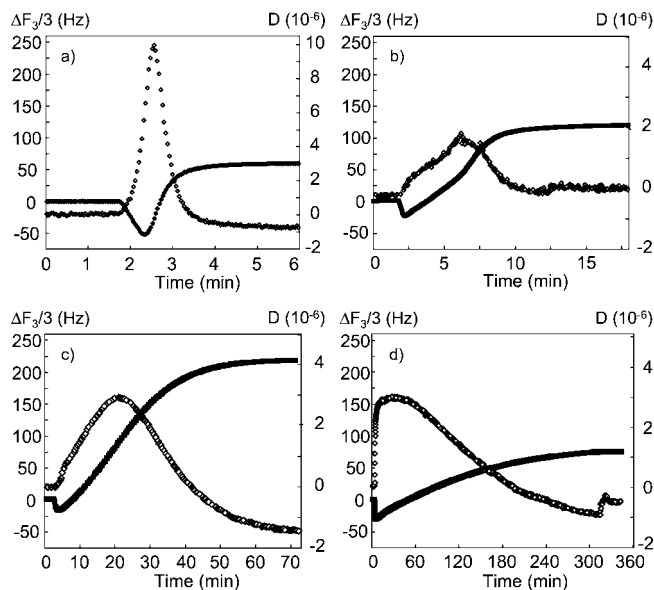


Figure 5. Change in frequency (f) and change in dissipation (D), for (a) NFC, (b) LS, (c) SC regenerated, and (d) NC cellulose model film treated with 0.5% cellulase mixture. The frequency and dissipation profiles are the normalized third overtones for a driving frequency of 15 MHz (40 °C and pH 5). Filled squares correspond to the frequency plot, and open diamonds correspond to energy dissipation.

case of the SC regenerated cellulose, is somewhat longer (more than 1 h, as seen in Figure 5c). As expected, the highly crystalline cellulose structure (film from cellulose nanocrystals) significantly slows down the enzymatic hydrolysis, and it is much more difficult for the structure to break down (see Figure 5d). The time required for depletion of the film is now 6 h compared to the typical few minutes required in the case of the nanofibril films or the LS films. The reason behind this is the strong hydrogen-bonding network, which makes crystalline cellulose resistant to enzymatic hydrolysis,³⁰ as reported in similar studies using different experimental approaches.^{6,7}

The energy dissipation increases during the hydrolysis as a result of increased viscoelasticity of the films, i.e., the cellulose layers are cleaved, and the film becomes more hydrated and swollen. Differences in model film topographies and the nature of cellulose contribute to the observed increased swelling (viscoelasticity) as a result of enzyme activity. A maximum in the energy dissipation curve is detected during the hydrolysis phase. In the case of the nanofibril film, this maximum occurs very early, usually within one minute after enzyme incubation. The observed (maximum) D value (10×10^{-6}) for the nanofibril film is very large compared to corresponding D values for the LS, SC, and NC films ($2\text{--}3 \times 10^{-6}$). This may further indicate that the nanofibrils are first liberated from the surface so that they protrude out into the solution. Thereafter the enzymes cleave the chains off the surface without a total conversion of the nanofibrils to sugars or oligomers. In the case of the LS and the SC surfaces, the maximum in energy dissipation occurs during the hydrolysis stage, before the degradation starts to slow down. The frequency at which this maximum occurs is closely related to the structure of the film, and has been considered a fingerprint of the morphological changes during enzymatic degradation.² In contrast with LS and SC surfaces, the maximum in energy dissipation for the NC film is found at an early stage of degradation. The nature of the cellulose film explains such a

(30) Nishiyama, Y.; Langan, P.; Chanzy, H. *J. Am. Chem. Soc.* **2002**, *124*, 9074–9082.

Table 3. Summary of Fitting Parameters (Eq 1 and 2) for Different Cellulose Films^a

film	NFC	LS	SC	NC
M_{MAX} (Hz)	-95	-52	-31	-29.6
τ (min ⁻¹)	0.7	0.7	1.9	0.5
B (Hz)	115	142	232	120
C (min ⁻¹)	0.45	1.6	6.1	132
$1/C$ (min)	2.22	0.62	0.16	<0.01

^a NFC = nanofibrillar cellulose; LS = Langmuir–Schaefer regenerated cellulose; SC = spin-coated regenerated cellulose; NC = cast cellulose nanocrystals. Experimental conditions were 40 °C and enzyme load of 0.5% v/v.

difference. The viscoelasticity of the NC film increases as proteins are adsorbed. EGs and certain CBHs with appropriate carbohydrate binding modules (CBMs) bind the crystalline surface.^{11,31–33} EGs start to cleave the superficial chains of the crystals, exposing open chains to facilitate exoglucanases work. The adsorption of more enzymes, the solvation of the open chains, and a minor diffusion of water to the newly exposed crystal surface explain that sudden increase in energy dissipation. The maximum in dissipation value is held for quite a long time (almost 60 min). Thereafter, the energy dissipation decreases as nanocrystals are hydrolyzed and the film thins out and becomes more rigid.

Modeling the QCM-D measurements was used to quantify and compare the kinetics of enzyme activity for the different substrates. Table 3 summarizes the average values for maximum binding (M_{MAX} and relaxation time τ) and the average values for hydrolysis (B and C) for the cellulose surfaces studied. As a reminder, M_{MAX} is related to the maximum amount of protein adsorbed; the relaxation time τ quantifies the (inverse of the) rate of binding; B denotes the maximum extent of hydrolysis, and C (or $1/C$ as the hydrolysis rate) allows comparison of the enzyme kinetics for the different cases.

In terms of the degradation rate, nanofibrillar cellulose films showed to be hydrolyzed the fastest, as was also observed from the QCM-D curves in Figure 5. However, as was pointed out before, the release of cellulose fractions instead of oligomeric hydrolysis may explain this observation. The degradation of the regenerated cellulose films was somewhat slower than the nanofibrillar cellulose films. The time to hydrolyze spin coated films was around 13 times longer compared to the nanofibril films. The LS cellulose films showed a hydrolysis rate ca. 4 times slower than that for nanofibril films.

The degree of crystallinity of the model cellulosic films is shown to critically affect the enzymatic hydrolysis rate. The most significant difference was obtained with the NC film. The hydrolysis rate indicated that the degradation was substantially slower compared to the rest of the films studied. The slow degradation kinetics of cellulose also reduces the overlap between the binding and the hydrolysis stages. In the case of NC films, a set of experimental data was used to fully describe binding dynamics (not shown). The enzymatic hydrolysis of the NC film took place at a low and constant rate during the experiment. This suggests that the cellulases encountered a substrate that was uniformly difficult to degrade.

Structural Changes in Different Cellulose Model Films after Enzymatic Hydrolysis. The morphological changes that occur in the different cellulose films upon enzymatic hydrolysis were studied by AFM imaging. Figure 6 shows AFM height

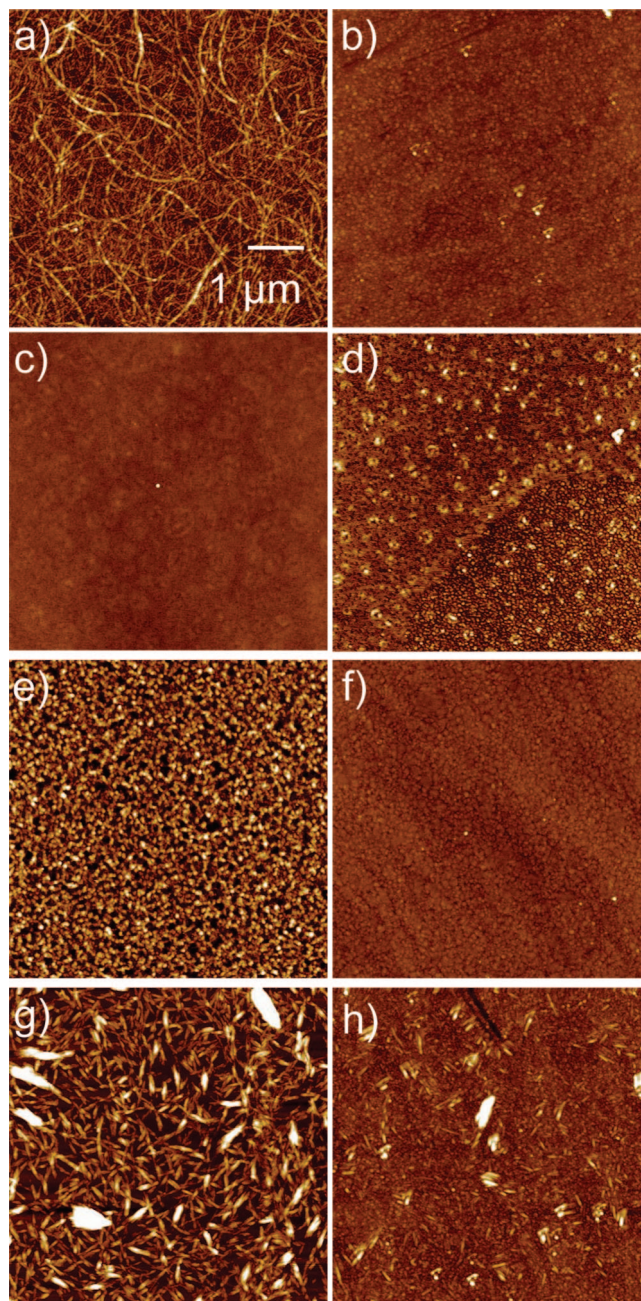


Figure 6. AFM height images of NFC film (a) before and (b) after enzymatic hydrolysis, LS-model film (c) before and (d) after hydrolysis, SC regenerated cellulose film (e) before and (f) after hydrolysis, and NC surface (g) before and (h) after hydrolysis. The scan size is $5 \times 5 \mu\text{m}$, and the Z-range is 30 nm, except for image g, where the Z-range is 50 nm.

images of cellulose nanofibril model film, LS regenerated cellulose film, SC regenerated cellulose film, and cast cellulose NC film (before and after the enzymatic incubation). The cellulose nanofibril film (Figure 6a) is removed after the hydrolysis (Figure 6b). The LS film (Figure 6c) is not completely degraded by the cellulases (Figure 6d). Two different regions can clearly be seen, indicating that the degradation of the film proceeds only partially, and the rest of the film can not be degraded by the cellulases. A possible explanation for this is the occurrence of recrystallization of regenerated cellulose to cellulose II due to self-assembly during the LS film preparation. The SC regenerated cellulose film (Figure 6e) is completely removed by the enzymes, and the typical structure of the substrate can be seen after the hydrolysis (Figure 6f). The NC surface (Figure 6g) is not fully degraded

(31) Linder, M.; Teeri, T. T. *J. Biotechnol.* **1997**, 57(9), 15–28.

(32) Koivula, A.; Kinnari, T.; Harjunpää, V.; Ruohonen, L.; Teleman, A.; Drakenberg, T.; Rouvinen, J.; Jones, T. A.; Teeri, T. T. *FEBS Lett.* **1998**, 429(6), 341–346.

(33) Linder, M.; Nevanen, T.; Teeri, T. T. *FEBS Lett.* **1999**, 447(3), 13–16.

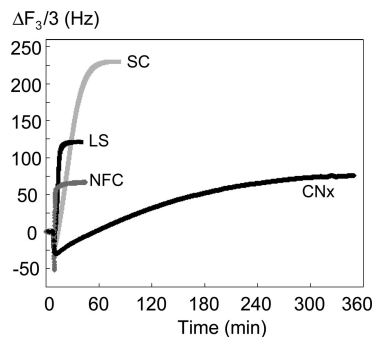


Figure 7. Change in frequency (Δf), for NFC, LS, SC, and NC cellulose model films treated with a 0.5% cellulase mixture (40 °C and pH 5).

(Figure 6h) and the (original) largest crystals remained on the substrate. This was expected because crystalline cellulose is more difficult to degrade than the amorphous cellulose.

A major difference between the studied films is the available surface area. While LS films are relatively flat (see Table 2 and Figure 6), the nanofibril films form three-dimensional networks with larger exposed surface area. This can affect the fast hydrolysis kinetics for the nanofibril film because the enzymes can reach more effectively the inner layers of the nanofibril network. In contrast to the nanofibril films, the enzymes bind more likely on the top layers of the LS films, and hence the degradation starts from the top down. For the SC film, the rms roughness suggests a slightly larger available surface area. However, we would like to point out that the rms roughness was determined for dry films in air. In water, the nanofibril film has a very open structure as indicated by earlier swelling and surface force measurements.²⁰ In contrast, although rougher than the LS film, the SC film is still rather compact, and the enzymatic degradation probably proceeds from the top down. The available surface area is very high for the NC film, but the high degree of crystallinity is, in this case, a more determining factor, causing an effective decrease in the hydrolysis rate.

Different substrates were also used for film formation. Nanofibril films were formed on APTS-treated silica crystals, LS films were formed on polystyrene-coated gold crystals, SC films were formed on PVAm-treated silica crystals, and NC surfaces were formed on gold sensors. However, these differences between the substrates are not expected to have significant influence on the enzymatic degradation of the cellulose films.

The thickness of the films is also a factor to consider. Due to the varying thicknesses (see Table 2), the films also have a varying degradable mass. The degradable mass of the model films affects the maximum frequency value (in Hz) that corresponds to the plateau region, once degradation is completed. Nanofibril, LS, and NC films have somewhat similar maximum frequency values, but the SC regenerated cellulose film has significantly higher maximum frequency, indicating that the degradable mass is the highest for the SC film. This is also observed from Figure 7, which shows, as a summary, QCM-D frequency curves after enzymatic incubation for all the films studied. The maximum frequency value in Hz is proportional to the degradable mass, and also to the time of the degradation. However, the initial rate of hydrolysis is not affected by the thickness of the films and the degradable mass, but it is determined by the nature of cellulose and architecture of the film.

Figure 7, which outlines all frequency curves on the same time scale, clearly indicates that the nature of cellulose strongly affects the enzymatic hydrolysis of cellulose films. By comparing different types of model films, factors contributing to enzyme activity can be understood more completely. The differences in hydrolysis kinetics for the various substrates highlight the importance of choosing the right substrate for any meaningful interpretation. It is evident that lignocellulosic biodegradation is a complex phenomenon that is intractable for experimentation when attempting to decouple the contributing effects (such as substrate morphology, crystallinity, chemistry, and accessibility). Striking differences in enzyme activities were found for the different cellulose films that were compared in this study. While the used cellulose films are simple models for real substrates, we show that chemical and morphological differences, which macroscopically may seem to be very subtle, play important roles in the overall time evolution of film degradation. Finally, QCM frequency and dissipation profiles in combination with AFM imaging after substrate incubation add to our understanding of enzyme adsorption and mechanism of action. Complementary efforts are being conducted by using pure enzymes. However, it is known that it is the combined effect of different cellulases that is responsible for maximum conversion rates in actual applications. While we used multicomponent enzymes and focused on their overall effect on different substrates, it is anticipated that the proposed protocols can be extremely useful in enzyme screening and in the optimization of enzyme formulations.

Conclusions

Model films of native cellulose nanofibrils, which contain both crystalline and amorphous cellulose, were used to investigate their enzymatic degradation by monitoring the changes in frequency and energy dissipation with a QCM. The rate of enzymatic degradation of the nanofibril films was very fast under the experimental conditions tested. AFM images of the cellulosic substrates (before and after enzymatic hydrolysis) revealed that the nanofibril film was completely removed after short degradation time.

The enzyme binding and substrate degradation observed in the case of nanofibril films were compared with three other types of models for cellulose, namely, LS and SC regenerated cellulose, and cellulose NC cast film. The nature of the cellulose substrate (crystallinity and morphology) markedly influenced the dynamics of enzymatic degradation.

Overall, our observations on the effect of cellulase enzymes on the various model films help to further elucidate the complex mechanisms involved in biomass biodegradation.

Acknowledgment. Financial support provided by the North Carolina Biotech Center (NCBC) under Grant NCBC #2007-CFG-8016, and Novozymes of North America, Inc. is gratefully acknowledged. Prof. Tom Lindström and M.Sc. Mikael Ankerfors at STFI-Packforsk, Sweden, are acknowledged for providing the nanofibril samples. Drs. Y. Kim and G. Montero are acknowledged for providing cellulose nanocrystals. M.Sc. Delphine Miquel is acknowledged for her help with nanofibril film preparation. The experimental assistance of Ritva Kivelä and Aila Rahkola is gratefully acknowledged.

LA801550J